PHYSICAL REVIEW A **94**, 013425 (2016)

Vibrationally resolved electron-nuclear energy sharing in above-threshold multiphoton dissociation of CO

Xufei Sun,[1] Min Li,[2] Yun Shao,[1] Ming-Ming Liu,[1] Xiguo Xie,[1] Yongkai Deng,[1]
Chengyin Wu,[1,3] Qihuang Gong,[1,3] and Yunquan Liu[1,3]
[1] *Department of Physics and State Key Laboratory for Mesoscopic Physics, Peking University, Beijing 100871, China*
[2] *Wuhan National Laboratory for Optoelectronics and School of Physics, Huazhong University of Science and Technology, Wuhan 430074, China*
[3] *Collaborative Innovation Center of Quantum Matter, Beijing 100871, China*
(Received 20 January 2016; published 26 July 2016)

We study the photon energy sharing between the photoelectron and the nuclei in the process of above-threshold multiphoton dissociative ionization of CO molecules by measuring the joint energy spectra. The experimental observation shows that the electron-nuclear energy sharing strongly depends on the vibrational state. The experimental observation shows that both the energy deposited to the nuclei of CO^+ and the emitted photoelectron decrease with increasing the vibrational level. Through studying the vibrationally resolved nuclear kinetic energy release and photoelectron energy spectra at different laser intensities, for each vibrational level of CO^+, the nuclei always tend to take the same amount of energy in every vibrational level regardless of the laser intensity, while the energy deposited to the photoelectron varies with respect to the laser intensity because of the ponderomotive shifted energy and the distinct dissociative ionization mechanisms.

DOI: 10.1103/PhysRevA.94.013425

I. INTRODUCTION

The photon energy transferring to atoms and molecules in strong laser fields has been an intriguing subject in optical physics and chemistry [1]. Exposing an atom in an intense laser field, the electron can absorb a certain number of photons more than required leading to a series of peaks separated by the photon energy in the photoelectron energy spectra, which is referred to as above-threshold ionization (ATI) [2]. Compared with atoms, the interaction of molecules with photons would be very complicated because the electronic, vibrational, rotational, and dissociative motions will be involved. The ionic fragments can share part of the photon energy with the electrons, which has been observed in single-photon dissociative ionization of molecules [3,4]. For molecules in ultrafast strong laser fields, many interesting and important phenomena have been studied, including bond softening [5], bond hardening [6,7], above-threshold dissociation [8], enhanced ionization [9,10], Coulomb explosion imaging [11–15] and their dynamics control [16–19], etc. Most of those works are done by separately measuring the energy or momentum spectra of the photoelectrons and the nuclei.

The correlation between the photoelectron and nuclei in strong-field multiphoton dissociative ionization of molecules is usually ignored in most of the early theoretical treatments. By investigating the joint energy spectrum (JES) [20–22], it has been theoretically shown that the correlation between the nuclei and electron in molecular dissociation cannot be neglected for multiphoton dissociation of ${H_2}^+$. Generally, the sum of the kinetic energy of nuclear fragments (E_N) and photoelectrons (E_e) after the end of the laser pulse, is given by $E_{\mathrm{sum}} = E_N + E_e = E_0 + n\omega - U_p$, where E_0 is the bound state energy, and U_p the ponderomotive energy (atomic units throughout, unless indicated otherwise). A recent experiment has verified the energy sharing of the absorbed photons between the photoelectron and the nuclei in above-threshold multiphoton dissociative ionization of the simplest molecule H_2 [23].

The JES spectra can provide rich information of strong-field dissociation ionization. Recently, inter- and intracycle interference effects have been theoretically identified in the JES spectra of multiphoton dissociation of ${H_2}^+$ [24]. The molecular rotational and vibrational effects are expected to be important for the correlated dynamics of strong-field dissociative ionization, which, however, have not been studied at all. On the other hand, the study of the energy sharing for multielectron molecules would be very necessary for an understanding of the underlying correlated strong-field molecular dissociative dynamics. In this work, we present an experimental observation of the vibrationally resolved electron-nuclear JES from above-threshold multiphoton dissociation of CO molecules in intense femtosecond laser pulses at different intensities. Through measuring the nuclear kinetic energy release (KER) spectra and angular distribution of molecular dissociation, we determine the laser-induced dissociation pathways contributing to the vibrationally resolved JES. For each vibrational level, the energy sharing between the nuclei and the photoelectron plays a significant different role in the dissociation process. The measured JES further shows that the nuclei always tend to take the same amount of energy regardless of the laser intensity, while the energy deposited to the photoelectron varies at different laser intensities.

II. EXPERIMENTAL SETUP

Experimentally, we used an ultraviolet (UV) laser pulse ($\lambda = 390$ nm) to study the correlated electron-nuclear dynamics of multiphoton molecular dissociation, which is produced from the frequency doubling of a near-infrared pulse (25 fs, 780 nm, 3 kHz) with a 200-μm-thick β-barium borate crystal. The UV laser pulse was focused onto a supersonic gas jet of CO by a concave mirror. In order to avoid the false coincidence event, we achieved the pressure as better as 5×10^{-11} mbar in the interaction chamber. The estimated gas density is $\sim 10^{11}/\mathrm{cm}^3$. We measured the three-dimensional

©2016 American Physical Society

momentum distributions of ions and photoelectrons using cold target recoil-ion momentum spectroscopy [25,26]. The dissociative fragments, i.e., ions and electron, were recorded in coincidence by two separated time- and position-sensitive microchannel plate delay-line detectors. By tracing the yields of CO^+ as an autocorrelation signal, the temporal duration of the UV pulse was characterized to be 50 fs.

III. RESULTS AND DISCUSSION

Figure 1(a) shows the measured JES for above-threshold multiphoton dissociation of CO exposed to the linearly polarized UV pulse at the intensity of 0.6×10^{14} W/cm^2. The pathway of this dissociation process is $CO + n\omega \rightarrow C^+ + O + e^-$ [referred to as CO(1,0) channel]. Experimentally, the correlated C^+ ions and photoelectrons from the CO(1,0) channel were measured in coincidence. We deduce the momentum of the neutral O atom using the momentum conservation law with all molecular dissociative fragments, as the absorbed and emitted photons have negligible momenta. The total energy deposited to the nuclei, i.e., the total nuclear KER, can be represented as $E_N = E_C^+ + E_O$. After integrating the JES over E_N and E_e, respectively, we obtain the corresponding energy spectra of the photoelectron E_e and nuclei E_N, as illustrated in Figs. 1(b) and 1(c).

The characteristic feature of the electron-nuclear JES is the diagonal lines which evidently reflect the sharing of the absorbed photon energy between the nuclei and photoelectron. More interestingly, the JES in Fig. 1 reveals much more than the general energy sharing feature. The unique feature is the discrete energy distribution along each JES line, which indicates the vibrational resolution when the nuclear wave packet dissociates from different vibrational states. As shown in Fig. 1(c), the equally discrete KER peaks of nuclei distribute in the range of 0–1.6 eV. In addition, the yields of the dissociative ionic fragments increase with the increasing vibrational level. Particularly, the yield sharply increases in $\upsilon'' = 5$, reaches the maximum at $\upsilon'' = 6$, and almost has no distribution above $\upsilon'' = 6$ vibrational level, indicating the over-barrier molecular dissociation limit. The vibrationally resolved electron-nuclear JES, to the best of our knowledge, has not been reported experimentally, thus raising the crucial question about the mechanism of the electron-nuclear energy sharing over different vibrational states.

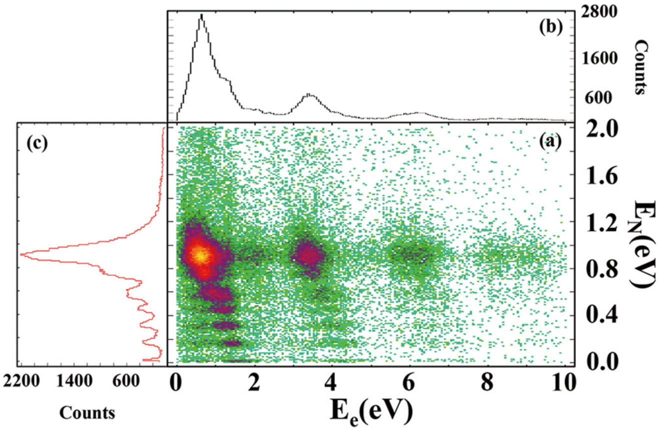

FIG. 1. (a) Electron-nuclear JES of above-threshold multiphoton dissociative ionization channel of CO(1,0) at an intensity of 0.6×10^{14} W/cm^2. (b) and (c) show the corresponding photoelectron energy spectrum and the nuclear KER spectrum, respectively.

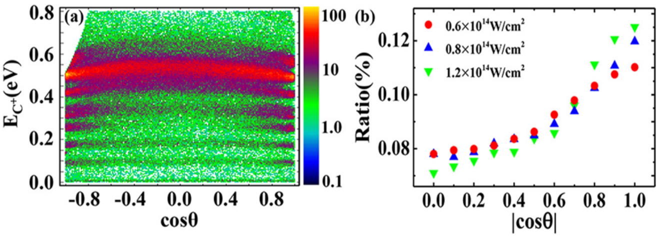

FIG. 2. (a) The angular distribution of the dissociative fragment C^+ at an intensity of 0.6×10^{14} W/cm^2. Here θ is the angle between the molecular axis and the direction of the laser polarization. (b) The ratio of both parallel and perpendicular transitions with respect to $|\cos\theta|$ at different laser intensities.

In order to understand the dynamics behind this mechanism, we first determine the laser-induced dissociation pathways of CO^+. We show the density distribution of C^+ KER with respect to $\cos\theta$ in Fig. 2(a), where θ is the angle between the laser polarization and the internuclear axis of CO^+. The transition involved in the dissociation pathway can be found by the change in the angular momentum quantum number $\Delta\Lambda$, i.e., the parallel transition $\Delta\Lambda = 0$ (e.g., $\sum \leftrightarrow \sum$, $\prod \leftrightarrow \prod$) and the perpendicular transition $\Delta\Lambda = \pm 1$ (e.g., $\sum \leftrightarrow \prod$). As shown in Fig. 2(a), the most distinct feature of the density plot is that the yield of the C^+ fragment both along and perpendicular to the laser polarization increase with the increasing vibrational level, indicating that the dissociation pathway must include both parallel and perpendicular transitions. Considering the angular distribution, we then show the contribution from both parallel and perpendicular transitions at different laser intensities in Fig. 2(b). One can find that for all laser intensities, the parallel transitions always dominate because of the permanent dipole. The relative contribution from the parallel to the perpendicular pathway becomes larger with increasing laser intensity. One cannot simply determine the number of photons emitted and absorbed in parallel and perpendicular transitions along the pathways, respectively, by a fitted $\cos^{2n}\theta \sin^{2m}\theta$ distribution [27,28]. We need consider the possible transitions to determine the dissociation pathways of CO.

The potential energy curves of the associated states of CO^+ are shown in Fig. 3(a). For the CO^+ ions produced by the vertical ionization of CO, most of the population is distributed at the two lowest electronic states, namely, the ground state $X\,^2\sum^+$ and the lowest-lying metastable state $A\,^2\prod$. One can attribute the transition pathways from the experimental observation. First, as seen by the nuclear KER spectrum in Fig. 1(c), the position and the spread of the nuclear KER generated by the associated pathways should distribute among a low KER range from 0 to ~ 1.6eV. Second, since the yield of the dissociative nuclear fragments increases slowly from $\upsilon'' = 0$ to $\upsilon'' = 4$, sharply increases at $\upsilon'' = 5$, and finally maximizes at $\upsilon'' = 6$ state, this indicates that the wave packets populating in low vibrational levels from $\upsilon'' = 0$ to $\upsilon'' = 4$ dissociate through a multiphoton process,

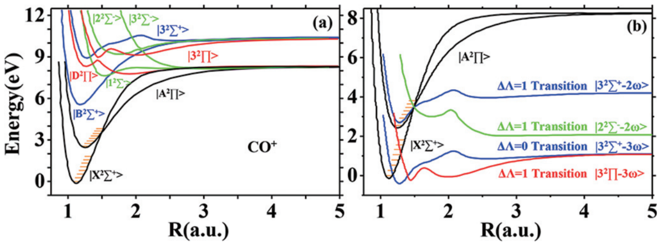

FIG. 3. (a) The potential energy curves of CO$^+$ (taken from [33]). The two possible initial electronic states involved in this experiment, $X\,{}^2\sum^+$ and $A\,{}^2\prod$, are labeled with the short lines referring to the vibrational levels. (b) Dressed-state diabatic states of CO$^+$. Lines with different color refer to different transition pathways contributing to vibrationally resolved KER (see text).

while the vibrational wave packet above $\upsilon'' = 4$ experiences an over-barrier dissociation. Thus, the crossing where the coupling of the $X\,{}^2\sum^+$ or $A\,{}^2\prod$ state with the dressed excited state should be near the high vibrational level such as $\upsilon'' = 4,5$, or there should be a barrier in the dressed state with the height around $\upsilon'' = 4,5$ at a certain internuclear distance.

Here we adopt the diabatic Floquet representation [29–32] to illustrate the coupling of different dressed states. For the parallel transition, the only possible pathway that can satisfy the above conditions is the three-photon pathway, i.e., $|X\,{}^2\sum^+ - 0\omega\rangle \rightarrow |3\,{}^2\sum^+ - 3\omega\rangle$, as shown in Fig. 3(b). The crossing of the ground state $|X\,{}^2\sum^+ - 0\omega\rangle$ coupling to the dressed $|3\,{}^2\sum^+ - 3\omega\rangle$ state is near $\upsilon'' = 1$, however, there is a barrier in the $|3\,{}^2\sum^+ - 3\omega\rangle$ state with the height between $\upsilon'' = 4$ and $\upsilon'' = 5$ level at an internuclear distance $R \sim 2.2$ a.u, while for the perpendicular transition, there is also one possible pathway. That is, the population of the $|X\,{}^2\sum^+ - 0\omega\rangle$ state between $\upsilon'' = 4$ and $\upsilon'' = 5$ couples to the dressed $|3\,{}^2\prod - 3\omega\rangle$ excited state, dissociating to the $|3\,{}^2\prod - 3\omega\rangle$ limit, i.e., $|X\,{}^2\sum^+ - 0\omega\rangle \rightarrow |3\,{}^2\prod - 3\omega\rangle$ pathway, as shown with the red line in Fig. 3(b). Other pathways, such as $|A\,{}^2\prod - 0\omega\rangle \rightarrow |2\,{}^2\sum^- - 2\omega\rangle$ and $|A\,{}^2\prod - 0\omega\rangle \rightarrow |3\,{}^2\sum^+ - 2\omega\rangle$ in Fig. 3(b), can produce the correct dissociative nuclear fragment yield, but they have the incorrect KER distribution. Although the height of the barrier in parallel transition and the crossing in perpendicular transition are in between that of the vibrational level $\upsilon'' = 4$ and $\upsilon'' = 5$, the height of the barrier is slightly higher than the crossing. This can explain why the relative yield from parallel to perpendicular transition becomes larger when laser intensity increases as seen in Fig. 2(b).

Having determined the possible dissociation pathways contributing to the vibrationally resolved JES, one can now investigate how the energy of photons is shared between the correlated nuclei and photoelectrons in different vibrational levels in multiphoton molecular dissociation. As illustrated in Fig. 3(b), two pathways have the same dissociation limit. The difference of the barrier height and the crossing is less than the energy interval of the adjacent vibrational level, and thus, they would reveal a similar energy sharing mechanism. Since the parallel pathway dominates, we take it as an example. We consider the two-step model, i.e., the nuclei instantaneously acquire a kinetic energy of E_{N0} from the interaction with the outgoing photoelectrons in the first vertical ionization step. Then they propagate along the coupled dissociation pathway, i.e., $|X\,{}^2\sum^+ - 0\omega\rangle \rightarrow |3\,{}^2\sum^+ - 3\omega\rangle$, and dissociate to the continuum of the $|3\,{}^2\sum^+ - 3\omega\rangle$ state, leading to the observable asymptotic nuclear KER E_N.

Inspecting JES of the first ATI peak in Fig. 1(a), one can find that the nuclear KER E_N increases with the increasing vibrational level, while the photoelectron energy E_e decreases when the vibrational level increases. In order to estimate how much photon energy is transferred to the nuclei in different vibrational levels in the first vertical ionization step, we extract the vibrational energy $E_{\upsilon''}$ from the $\upsilon'' = 0$ to $\upsilon'' = 6$ state [33,34]. Based on the two-step model, we have $\Delta E = E_{\upsilon''} - E_{g0}$ and $E_{N0} = E_N - \Delta E$, where $E_{g0} = 1.078$ eV is the dissociation limit of the $|3\,{}^2\sum^+ - 3\omega\rangle$ state as illustrated in Fig. 3(b), and ΔE is the energy acquired when the vibrational wave packet propagates along the $|X\,{}^2\sum^+ - 0\omega\rangle \rightarrow |3\,{}^2\sum^+ - 3\omega\rangle$ pathway to the end of the dissociation. As a result, the vibrational level higher than the dissociation limit will acquire the extra energy during the dissociation, while the vibrational level lower than the dissociation limit will consume the energy from E_{N0}, which is deposited in the nuclei of CO$^+$, to accomplish dissociation.

The analytical results are shown in the Table I. One can find that the vibrational energy of $\upsilon'' = 5,6$ is higher than E_{g0}, so the vibrational wave packet acquires an extra energy during the dissociation process, i.e., $\Delta E > 0$. In contrast, the energy of $\upsilon'' = 0–4$ is lower than E_{g0}, and as a result the wave packet will consume energy from E_{N0}, i.e., $\Delta E < 0$. This means that

TABLE I. Experimental and analytical results of electron-nuclear energy sharing in different vibrational levels of the $X\,{}^2\sum^+$ state at an intensity of 0.6×10^{14} W/cm^2.

υ''	0	1	2	3	4	5	6
E_N(eV)	0.01	0.165	0.31	0.45	0.575	0.775	0.9
E_e(eV)	1.575	1.465	1.335	1.225	1.025	0.725	0.625
$E_{\upsilon''}$(eV)	0.0	0.265	0.531	0.796	1.061	1.326	1.562
FC factor[a]	9.64×10^{-1}	3.59×10^{-2}	1.03×10^{-4}	1.96×10^{-6}	2.20×10^{-10}	3.44×10^{-10}	4.00×10^{-12}
ΔE(eV)	−1.078	−0.813	−0.547	−0.282	−0.017	0.248	0.484
E_{N0}(eV)	1.088	0.978	0.857	0.732	0.592	0.527	0.416
$\lvert\Delta E_{N0}\rvert$(eV)($\lvert E_{N0(\upsilon'')} - E_{N0(\upsilon''-1)}\rvert$)		0.11	0.121	0.125	0.14	0.065	0.111
$\Delta E_{\upsilon''}$(eV)($E_{\upsilon''} - E_{\upsilon''-1}$)		0.271	0.267	0.263	0.259	0.256	0.252

[a] Reference [35].

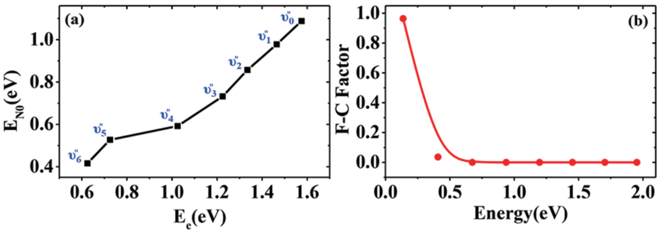

FIG. 4. (a) The energy deposited to the nuclei of CO$^+$ (E_{N0}) with respect to the photoelectrons E_e in different vibrational levels. (b) Frank-Condon factors (CO $X\ ^1\sum^+, \upsilon' = 0 \rightarrow$ CO$^+$ $X\ ^2\sum^+, \upsilon'' =$ 0−7 as a function of vibrational energy $E_{\upsilon''}$).

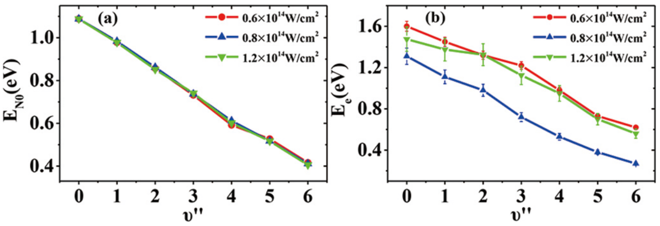

FIG. 5. The energy deposited to (a) the nuclei of CO$^+$(E_{N0}) and (b) the emitted photoelectron (E_e) in different vibrational levels at different laser intensities.

the sharing nuclear energy E_{N0} for the wave packet populated in $\upsilon'' = 5,6$ are all stored in the nuclear KER E_N. However, a part of E_{N0} for $\upsilon'' = 0-4$ is consumed in the dissociation process and the rest of them will be reserved in E_N. Therefore, the E_{N0} of different vibrational levels where the nuclear wave packets are populated plays a significant different role in the succeeding dissociation process.

According to the measured E_N in different vibrational levels, we estimate the corresponding energy E_{N0} with respect to E_e with respect to the vibration level, as illustrated in Fig. 4(a). Contrary to E_N, both E_{N0} and E_e decrease with the increasing vibrational level. This is because the lower vibrational level needs more energy to consume in the dissociation process. The electron has to transfer more energy to the nuclei of CO$^+$ for the lower vibrational level. The energy difference of E_{N0} of adjacent vibrational levels, i.e., $|\Delta E_{N0}|$, is smaller than the energy difference of the remaining energy of them, i.e., the energy interval of adjacent vibrational levels $\Delta E_{\upsilon''}$. Since $\Delta E_{\upsilon''}$ includes $|\Delta E_{N0}|$ and the electron energy difference, the electron energy decreases with the increasing vibrational level to compensate the extra energy difference of $\Delta E_{\upsilon''}$.

As seen by the Franck-Condon transition factor in Fig. 4(b) (data taken from [35]), the most populated state is expected to be the ground state of CO$^+$. This is in contrast with the measured KER, indicating strong coupling of the molecular dissociation in the laser field beyond the simple vertical transition. The correlated motion in vibrational states determines the electron-nuclear energy sharing and the succeeding dissociative dynamics in strong laser fields.

Figure 5 shows the distribution of E_{N0} and E_e with respect to the vibrational levels at different laser intensities. For all laser intensities in Fig. 5(a), E_{N0} decreases with the increasing vibrational level. Note that since the E_{N0} distribution does not change at different laser fields, the nuclei tend to take the same amount of energy while the electron tends to take all energy from the excess photons. Interestingly, the photoelectron energy E_e for each vibrational level is very sensitive to the laser intensity, as shown in Fig. 5(b). At intensities of 0.6×10^{14} W/cm^2 and 1.2×10^{14} W/cm^2, the photoelectron energy E_e for each vibrational level is higher than that of 0.8×10^{14} W/cm^2. The internuclear-dependent dissociation via the vibrational states can take place through the tunneling or over-the-barrier dissociation at different intensity. On the other hand, at different intensities, the vibrational states have different ac-Stark shifted energy. Both effects would play an important part in the energy sharing between the photoelectrons and the nuclei in strong-field molecular dissociation. The observation indicates complicated coupling of the vibrational states with the laser fields.

IV. CONCLUSION

In summary, we have experimentally investigated the vibrationally resolved electron-nuclear dynamics in above-threshold multiphoton dissociative ionization of CO molecules. The photon energy sharing of multielectron molecules is more complicated than $H_2{}^+$ and H_2. Because of the strong coupling of the vibrational states with the laser fields for CO molecules, the nuclei of CO$^+$ in higher vibrational levels acquire less photon energy compared with the nuclei at low vibrational states. The excess photon energy deposited to the photoelectron decreases with the increasing vibrational level. The energy sharing dynamics is sensitive to the laser intensity due to the ac-Stark shifted vibrational levels. The results would have important implications on the energy sharing dynamics of the strong-field multielectron molecular dissociation process.

ACKNOWLEDGMENTS

This work is supported by the National Program on Key Basic Research Project (Grant No. 2013CB922403) and the National Science Foundation of China (Grants No. 11434002 and No. 11125416). We thank Prof. J. Wu for the fruitful discussion.

---

[1] K. K. Lehmann and G. Scoles, Annu. Rev. Phys. Chem. **45**, 241 (1994).

[2] P. Agostini, F. Fabre, G. Mainfray, G. Petite, and N. K. Rahman, Phys. Rev. Lett. **42**, 1127 (1979).

[3] A. Lafosse, M. Lebech, J. C. Brenot, P. M. Guyon, O. Jagutzki, L. Spielberger, M. Vervloet, J. C. Houver, and D. Dowek, Phys. Rev. Lett. **84**, 5987 (2000).

[4] F. Martín, J. Fernández, T. Havermeier, L. Foucar, Th. Weber, K. Kreidi, M. Schöffler, L. Schmidt, T. Jahnke, O. Jagutzki, A. Czasch, E. P. Benis, T. Osipov, A. L. Landers, A. Belkacem, M. H. Prior, H. Schmidt-Böcking, C. L. Cocke, and R. Dörner, Science **315**, 629 (2007).

[5] P. H. Bucksbaum, A. Zavriyev, H. G. Muller, and D. W. Schumacher, Phys. Rev. Lett. **64**, 1883 (1990).

[6] A. D. Bandrauk and M. L. Sink, J. Chem. Phys. **74**, 1110 (1981).
[7] A. Zavriyev, P. H. Bucksbaum, J. Squier, and F. Saline, Phys. Rev. Lett. **70**, 1077 (1993).
[8] A. Giusti-Suzor, X. He, O. Atabek, and F. H. Mies, Phys. Rev. Lett. **64**, 515 (1990).
[9] T. Zuo and A. D. Bandrauk, Phys. Rev. A **52**, R2511 (1995).
[10] E. Constant, H. Stapelfeldt, and P. B. Corkum, Phys. Rev. Lett. **76**, 4140 (1996).
[11] Th. Ergler, A. Rudenko, B. Feuerstein, K. Zrost, C. D. Schröter, R. Moshammer, and J. Ullrich, Phys. Rev. Lett. **95**, 093001 (2005).
[12] J. H. Posthumus, L. J. Frasinski, A. J. Giles, and K. Codling, J. Phys. B **28**, L349 (1995).
[13] Th. Ergler, A. Rudenko, B. Feuerstein, K. Zrost, C. D. Schröter, R. Moshammer, and J. Ullrich, Phys. Rev. Lett. **97**, 193001 (2006).
[14] B. Manschwetus, T. Nubbemeyer, K. Gorling, G. Steinmeyer, U. Eichmann, H. Rottke, and W. Sandner, Phys. Rev. Lett. **102**, 113002 (2009).
[15] C. Wu, C. Wu, D. Song, H. Su, Y. Yang, Z. Wu, X. Liu, H. Liu, M. Li, Y. Deng, Y. Liu, L. Y. Peng, H. Jiang, and Q. Gong, Phys. Rev. Lett. **110**, 103601 (2013).
[16] M. F. Kling, Ch. Siedschlag, A. J. Verhoef, J. I. Khan, M. Schultze, Th. Uphues, Y. Ni, M. Uiberacker, M. Drescher, F. Krausz, and M. J. J. Vrakking, Science **312**, 246 (2006).
[17] M. Kremer, B. Fischer, B. Feuerstein, V. L. B. de Jesus, V. Sharma, C. Hofrichter, A. Rudenko, U. Thumm, C. D. Schröter, R. Moshammer, and J. Ullrich, Phys. Rev. Lett. **103**, 213003 (2009).
[18] Y. Liu, X. Liu, Y. Deng, C. Wu, H. Jiang, and Q. Gong, Phys. Rev. Lett. **106**, 073004 (2011).
[19] M. Li, P. Zhang, S. Luo, Y. Zhou, Q. Zhang, P. Lan, and P. Lu, Phys. Rev. A **92**, 063404 (2015).
[20] C. B. Madsen, F. Anis, L. B. Madsen, and B. D. Esry, Phys. Rev. Lett. **109**, 163003 (2012).
[21] R. E. F. Silva, F. Catoire, P. Rivière, H. Bachau, and F. Martín, Phys. Rev. Lett. **110**, 113001 (2013).
[22] Z. Wang, M. Li, Y. Zhou, Y. Li, P. Lan, and P. Lu, Phys. Rev. A **93**, 013418 (2016).
[23] J. Wu, M. Kunitski, M. Pitzer, F. Trinter, L. P. H. Schmidt, T. Jahnke, M. Magrakvelidze, C. B. Madsen, L. B.Madsen, U. Thumm, and R. Dörner, Phys. Rev. Lett. **111**, 023002 (2013).
[24] L. Yue and L. B. Madsen, Phys. Rev. A **93**, 031401(R) (2016).
[25] R. Dörner, V. Mergel, O. Jagutzki, L. Spielberger, J. Ullrich, R. Moshammer, and H. Schmidt-Böcking, Phys. Rep. **330**, 95 (2000).
[26] J. Ullrich, R. Moshammer, A. Dorn, R. Dörner, L. Ph. H. Schmidt, and H. Schmidt-Böcking, Rep. Prog. Phys. **66**, 1463 (2003).
[27] A. M. Sayler, P. Q. Wang, K. D. Carnes, B. D. Esry, and I. Ben-Itzhak, Phys. Rev. A **75**, 063420 (2007).
[28] J. McKenna, A. M. Sayler, B. Gaire, N. G. Johnson, E. Parke, K. D. Carnes, B. D. Esry, and I. Ben-Itzhak, Phys. Rev. A **77**, 063422 (2008).
[29] J. H. Shirley, Phys. Rev. **138**, B979 (1965).
[30] S.-I. Chu, J. Chem. Phys. **75**, 2215 (1981).
[31] T. F. George, J. Phys. Chem. **86**, 10 (1982).
[32] X. He, O. Atabek, and A. Giusti-Suzor, Phys. Rev. A **38**, 5586 (1988).
[33] K. Okada and S. Iwata, J. Chem. Phys. **112**, 1804 (2000).
[34] P. H. Krupenie and S. Weissman, J. Chem. Phys. **43**, 1529 (1965).
[35] R. W. Nicholls, J. Phys. B **1**, 1192 (1968).